Ground and Low-Lying States of Cu²⁺−H₂O. A Difficult Case for Density Functional Methods

J. Poater,[†] M. Solà,[†] A. Rimola,[‡] L. Rodríguez-Santiago,[‡] and M. Sodupe*,[‡]

Institut de Química Computacional and Departament de Química, Universitat de Girona, E-17071 Girona, Catalonia, Spain, and Departament de Química, Universitat Autònoma de Barcelona, Bellaterra 08193, Spain

The ground and low-lying states of Cu²⁺−H₂O have been studied using different density functional and post-Hartree−Fock methods. CCSD(T) results indicate that Cu²⁺−H₂O has C_{2v} symmetry and that the ground electronic state is a ²A₁ state. At this level of theory the relative order of the electronic states is ²A₁ < ²B₁ < ²B₂ < ²A₂. However, density functional results show that the relative stabilities of these states vary depending on the degree of mixing of exact Hartree−Fock (HF) and density functional (DF) exchange. For pure generalized gradient approximation (GGA) functionals and also for hybrid functionals with percentages of HF mixing up to ∼20−25%, the ²B₁ state becomes more stable than the ²A₁ one. Moreover, with these functionals a C_s(²A′) structure is found to be the ground-state structure of Cu²⁺−H₂O. This is attributed to the fact that, for C_{2v}(²B₁) and C_s(²A′), GGA functionals provide a delocalized picture of the electron hole, which is overstabilized due to a bad cancellation of the self-interaction part by the exchange-correlation functional. Among the different functionals tested, the one that provides better results compared to CCSD(T) is the BHLYP one.

I. Introduction

Gas-phase metal ion chemistry has experienced a tremendous growth in the past two decades.[1] This is partly due to the fact that the knowledge of the intrinsic properties of transition metal containing systems is of great importance in many fields such as catalysis, organometallics, and biochemistry. Moreover, studies on many metal−(L)ₙ systems have largely contributed to the understanding of metal ion solvation processes.[1,2] Many of the performed studies, however, have been devoted to singly positive charged metal complexes,[1] even though M²⁺ doubly charged metal ions are particularly important in chemistry and biochemistry. Gas phase studies of doubly charged M²⁺−L complexes are less common because they are more difficult to generate, due to charge-transfer dissociation processes or proton-transfer reactions.[3−6] Parallel to the experimental studies, many theoretical works on metal−ligand systems have dealt with singly positive cations.[1,7−10] These studies have provided important insights on the nature of metal−ligand interactions and on periodic properties as a function of the ground electronic state of the metal ion.[7] Moreover, the comparison with available experimental data has allowed calibration of the reliability of many theoretical approaches, especially that of the cost-effective density functional methods.[8−10] In contrast, theoretical studies on dications[11−13] are scarcer and the performance of density functional methods has been much less analyzed.

The existence of Cu²⁺−H₂O in the gas phase has been the subject of a recent controversy.[14,15] Previous pickup experiments indicated that Cu²⁺−(H₂O)₃ was the smallest stable cluster in gas phase.[16] However, a theoretical study of El-Hahas et al. showed that, although Cu²⁺−H₂O is unstable with respect to the charge separation asymptote, Cu⁺ + H₂O⁺, it is kinetically stable by a Coulomb energy barrier of about 7 kcal/mol.[17]

Recently, new mass spectrometry experiments have confirmed that Cu²⁺−H₂O can be generated as a long-lived dication.[18,19] The theoretical study of El-Nahas provided very valuable information on the stability of Cu²⁺−H₂O.[17] Nevertheless, the lowest electronic state of this complex was not reported and the ground-state structure, optimized with B3LYP, was found to have C_s symmetry,[17] in contrast to Cu⁺−H₂O[20] and most Mⁿ⁺−H₂O systems[11] which present C_{2v} symmetry, as expected considering that the planar structure provides the optimal ion−dipole interaction. On the other hand, previous results at the MP2(Full)/6-311++G(d,p) level have found Cu²⁺−H₂O to be planar.[11]

In this work we present a theoretical study of the ground and low-lying states of Cu²⁺−H₂O using density functional theory (DFT), Hartree−Fock (HF), and post-Hartree−Fock (post-HF) methods. We will show that the determined ground electronic state of Cu²⁺−H₂O changes depending on the functional considered. This is due to the fact that, in certain electronic states, there is an important charge and spin delocalization and these situations, as for two center−three electron bond systems,[21] have been found to be overstabilized with present density functionals. Our results also demonstrate that the relative stability of the different electronic states strongly depends on the degree of mixing of exact HF and DFT exchange functional.

A number of papers have addressed the effect of varying the fraction of exact HF exchange included in hybrid DFT functionals on molecular structure,[22−26] vibrational frequencies,[25] first-order density,[27,28] thermochemistry and energy barriers,[22,29−32] ionization potentials,[33] hydrogen bond infrared signature,[34] and nuclear resonance shielding constants.[35] Furthermore, Reiher and co-workers[36] have analyzed the importance of the admixture of exact HF exchange in the functional on the relative energy between states of different multiplicities. These authors have shown that high-spin states in Fe(II) transition metal complexes

---

[†] Universitat de Girona.
[‡] Universitat Autònoma de Barcelona.

Ground and Low-Lying States of Cu^{2+}−H$_2$O

J. Phys. Chem. A, Vol. 108, No. 28, 2004 **6073**

are stabilized when the degree of exact HF exchange is increased and that the energy splitting between low-spin and high-spin states depends linearly on the coefficient of the HF exchange admixture. According to the authors, the fact that HF includes Fermi correlation through exact exchange but not Coulomb correlation explains the overstabilization of high-spin states upon enlarging the amount of exact exchange admixture. In the present work, we report a clear example in which, for a series of same-spin low-lying electronic states, the determined ground electronic state depends on the degree of exact HF exchange included in the functional.

II. Methods

The geometries, energies, and harmonic vibrational frequencies of the $^2A_1$, $^2B_1$, $^2B_2$, and $^2A_2$ electronic states of the Cu^{2+}−H$_2$O system have been obtained within the unrestricted formalism using HF, post-HF, and density functional based methods.

Post-HF calculations have been performed using the coupled cluster singles and doubles method[37] including the effect of triple excitations by perturbation theory, CCSD(T),[38] and correlating all the electrons except the 1s electrons of O and the 1s, 2s, and 2p electrons of Cu. Two basis sets (hereafter referred as B1 and B2) have been used. In B1, the Cu basis set is based on the (14s9p5d) primitive set of Wachters[39] supplemented with one s, two p, and one d diffuse functions[40] as well as one f polarization function,[41] so that the final contracted basis set is [10s7p4d1f], whereas for O and H we have used the 6-311++G(d,p) basis. In the larger B2 basis set, the 6-311++G(3df,2pd) basis set is employed for O and H.

The same basis sets have been used for the calculations with the different functionals tested in the present work. For the correlation functional we have used the Lee, Yang, and Parr (LYP)[42] functional combined with two pure exchange functionals: Becke's 1988 functional (B)[43] and the 1996 exchange functional of Gill (G96).[44] In addition, two nonlocal hybrid exchange functionals, Becke's three parameter (B3)[45] and Becke's half-and-half (BH)[46] functionals, have been also combined with the LYP correlation functional.[42]

The B3 method was originally formulated as[45]

$$E_{XC} = E_{XC}^{LSDA} + a_o(E_X^{exact} - E_X^{LSDA}) + a_x \Delta E_X^{B88} + a_c \Delta E_C^{PW91} \tag{1}$$

The E_X^{exact}, E_{XC}^{LSDA}, ΔE_X^{B88}, and ΔE_C^{PW91} terms are the HF exchange energy based on Kohn−Sham orbitals, the uniform electron gas exchange-correlation energy, Becke's 1988 gradient correction for exchange,[43] and the 1991 Perdew and Wang gradient correction to correlation,[47] respectively. Commonly, this procedure is referred to as the B3PW91 method. The coefficients a_o, a_x, and a_c were determined by Becke[45] by a linear least-squares fit to 56 experimental atomization energies, 42 ionization potentials, and 8 proton affinities. The values thus obtained were a_o = 0.20, a_x = 0.72, and a_c = 0.81. In the Gaussian 98[48] implementation, the expression of the B3LYP functional is similar to eq 1 with some minor differences:[49]

$$E_{XC} = E_X^{LSDA} + a_o(E_X^{exact} - E_X^{LSDA}) + a_x \Delta E_X^{B88} + E_C^{VWN} + a_c(\Delta E_C^{LYP} - E_C^{VWN}) \tag{2}$$

In this equation, the Perdew and Wang correlation functional originally used by Becke is replaced by the Lee−Yang−Parr (LYP)[42] one. Since the LYP functional already contains a local part and a gradient correction, one has to remove the local part to obtain a coherent implementation. This can be done in an

approximate way by subtracting E_C^{VWN} from ΔE_C^{LYP}. Note that in the Gaussian 98 implementation the VWN functional is the one derived by Vosko et al. from a fit to the random phase approximation[50] results. Becke's half-and-half method (BHLYP)[46] also makes use of eq 1 with a_o = 0.5, a_x = 0.5, and a_c = 1. It is also worth noting that the set of parameters a_o = 1.0, $a_x = a_c$ = 0 does not reproduce the HF results due to the presence of the E_C^{VWN} term in eq 2.

Besides these functionals, another one has been tested, the hybrid MPW1PW91 functional, which combines the one-parameter modified Perdew−Wang exchange functional of Barone[51] (with a 25% exact exchange) and the Perdew−Wang 91 correlation functional.[47]

It is known that, for a given atomic electronic configuration, currently used functionals are not invariant over the set of densities associated with a degenerate atomic state, which implies that different occupancies corresponding to the same pure atomic state can lead to different energies.[52] In the present work, the Cu^{2+}−H$_2$O binding energy has been computed considering the orbital occupation of Cu^{2+} that leads to the lowest atomic energy. All calculations of geometries, energies, and vibrational frequencies have been performed with the Gaussian 98 package program.[48]

Finally, calculations of delocalization indices have been carried out by means of the AIMPAC collection of programs[53] using the following expression:[54−56]

$$\delta(A,B) = 2\sum_{i,j} S_{ij}(A) \, S_{ij}(B) \tag{3}$$

The summations in eq 3 run over all the occupied molecular spin−orbitals. $S_{ij}(A)$ stands for the overlap between molecular spin orbitals i and j within the basin of atom A. The delocalization index, $\delta(A,B)$, corresponds to the number of electrons delocalized or shared between atoms A and B.[54−56] The accuracy of the integrations for any molecule can be assessed by checking that the summation of all the localization and delocalization indices is equal to the number of electrons in the molecule. For all the molecules, the difference is always smaller than 10^{-3} au.

III. Results and Discussion

Cu^{2+} has a ^{2}D (d^9) electronic ground state. When interacting with water, the five d orbitals split, which leads to different low-lying electronic states depending on the metal d occupation. Although the energy order of these states is largely determined by the different overlap of the five d orbitals with H$_2$O, other factors such as 4s−3d and 4p−3d mixing or charge-transfer processes can also contribute to determining the ground state of Cu^{2+}−H$_2$O. Thus, assuming C_{2v} symmetry, we have performed geometric optimizations and frequency calculations for Cu^{2+}−H$_2$O in different symmetry electronic states. Table 1 shows the relative energies and Table 2 the optimized geometric parameters obtained with various density functionals as well as with the highly correlated CCSD(T) post-HF method.

B3LYP results show that, in the $^2A_1$ state, the singly occupied orbital mainly corresponds to the antibonding combination of the metal (4s−3d$_{z^2}$)(a$_1$) orbital with the 3a$_1$ one of H$_2$O. The (4s−3d$_{z^2}$) mixing is produced to reduce metal−ligand repulsion. In the $^2B_1$ state the open shell orbital is an antibonding combination of the metal 3d$_{yz}$(b$_1$) with the lone pair 1b$_1$ orbital of water, whereas in the $^2B_2$ electronic state, the open shell orbital is mainly centered on Cu^{2+} and corresponds to the 3d$_{xz}$(b$_2$) with a small (antibonding) contribution of the 1b$_2$ orbital

6074 *J. Phys. Chem. A, Vol. 108, No. 28, 2004*

Poater et al.

TABLE 1: Relative Energies (in kcal/mol) of the Ground and Low-Lying Electronic States of $Cu^{2+}-H_2O$ at Different Levels of Theory with Basis B1 (B2)

symmetry	state	G96LYP	BLYP	B3LYP	MPW1PW91	BHLYP	CCSD(T)[a]
C_{2v}	$^2A_1$	0.0 (0.0)	0.0 (0.0)	0.0 (0.0)	0.0 (0.0)	0.0 (0.0)	0.0 (0.0)
C_s	$^2A'$	−10.9 (−10.2)	−11.1 (−10.4)	−3.7 (−3.4)	−1.8 (−1.7)		
C_{2v}	$^2B_1$	−10.5 (−9.5)[b]	−10.7 (−9.8)[b]	−2.3 (−1.4)	0.7 (1.5)	6.6 (6.9)	5.6 (6.2)
C_{2v}	$^2B_2$	23.9 (23.8)	23.4 (23.3)	18.4 (18.4)	17.6 (17.7)	13.2 (13.4)	13.7 (13.9)
C_{2v}	$^2A_2$	28.5 (28.7)	27.8 (27.9)	21.2 (21.5)	20.3 (20.7)	15.7 (16.1)	16.3 (16.7)

[a] Values with the B2 basis set are obtained from single point calculations at the optimized CCSD(T)/B1 geometry. [b] First-order saddle point. See text.

TABLE 2: Optimized Geometric Parameters of $Cu^{2+}-H_2O$ in Different Electronic States with Basis B1 (B2)[a]

symmetry	state	geometry	G96LYP	BLYP	B3LYP	MPW1PW91	BHLYP	CCSD(T)
C_{2v}	$^2A_1$	R_{Cu-O}	1.874 (1.861)	1.878 (1.866)	1.844 (1.834)	1.832 (1.823)	1.837 (1.828)	1.841
		R_{O-H}	0.998 (0.995)	1.000 (0.997)	0.987 (0.985)	0.982 (0.979)	0.974 (0.971)	0.980
		α_{CuOH}	122.5 (122.7)	122.5 (122.7)	124.0 (124.1)	124.3 (124.5)	125.3 (125.4)	125.3
C_s	$^2A'$	R_{Cu-O}	1.976 (1.960)	1.983 (1.964)	1.898 (1.881)	1.866 (1.852)		
		R_{O-H}	1.006 (1.004)	1.009 (1.006)	0.994 (0.992)	0.987 (0.984)		
		α_{CuOH}	124.1 (123.5)	124.3 (123.7)	123.0 (122.4)	122.6 (121.9)		
		δ_{CuOHH}	157.9 (154.0)	158.8 (155.0)	152.3 (149.3)	150.8 (147.7)		
C_{2v}	$^2B_1$	R_{Cu-O}	1.988 (1.968)[b]	1.993 (1.971)[b]	1.917 (1.900)	1.891 (1.875)	1.862 (1.852)	1.865
		R_{O-H}	1.007 (1.005)[b]	1.009 (1.001)[b]	0.996 (0.993)	0.990 (0.986)	0.976 (0.973)	0.984
		α_{CuOH}	126.1 (126.2)[b]	126.1 (126.2)[b]	126.1 (126.2)	126.2 (126.3)	126.1 (126.2)	126.2
C_{2v}	$^2B_2$	R_{Cu-O}	1.910 (1.897)	1.913 (1.901)	1.908 (1.896)	1.904 (1.890)	1.909 (1.897)	1.919
		R_{O-H}	1.002 (0.999)	1.003 (1.000)	0.986 (0.982)	0.980 (0.977)	0.972 (0.970)	0.979
		α_{CuOH}	127.1 (127.2)	127.0 (127.1)	126.0 (12 6.2)	126.1 (126.2)	126.1 (126.2)	126.3
C_{2v}	$^2A_2$	R_{Cu-O}	1.926 (1.913)	1.929 (1.916)	1.917 (1.905)	1.911 (1.898)	1.911 (1.900)	1.922
		R_{O-H}	0.990 (0.988)	0.992 (0.989)	0.982 (0.980)	0.978 (0.975)	0.971 (0.968)	0.978
		α_{CuOH}	125.1 (125.4)	125.0 (125.3)	125.5 (125.7)	125.7 (125.9)	125.9 (126.0)	126.2

[a] Distances are in angstroms and angles are in degrees. [b] First-order saddle point. See text.

of H_2O. Finally, the singly occupied orbital in the $^2A_2$ state corresponds to the metal $3d_{xy}(a_2)$. This $^2A_2$ state is expected to be very similar to the $^2A_1$ state derived from monoccupying the $3d_{x^2-y^2}(a_1)$ orbital. It should be noted that the ligand contribution to the a_1 or b_1 singly occupied molecular orbitals decreases with the admixture of exact exchange in the functional (see below).

It can be observed in Table 1 that, at the CCSD(T) level of calculation, the ground electronic state of $Cu^{2+}-H_2O$ is the $^2A_1$ one, in agreement with previous calculations at the MP2 and CCSD(T) levels of theory.[11] This was to be expected considering that the $3d_{z^2}$ orbital is the one with a larger overlap with H_2O, and thus, doubly occupying the $3d_{xy}(a_2)$, $3d_{xz}(b_2)$, $3d_{yz}(b_1)$, and $3d_{x^2-y^2}(a_1)$ orbitals and maintaining the $3d_{z^2}(a_1)$ orbital singly occupied minimize the $Cu^{2+}-H_2O$ repulsion. At this level of theory, the relative stability of the different electronic states is $^2A_1 < ^2B_1 < ^2B_2 < ^2A_2$, in agreement with what one would expect considering the different overlap between the five d orbitals of the metal and H_2O.[57] That is, electronic states become increasingly less stable if metal d electrons are allocated in orbitals that have a larger overlap with H_2O, since then metal−ligand repulsion becomes larger. Accordingly, the R_{Cu-O} distance in the different electronic states follows the same trend: $R_{Cu-O}(^2A_1) < R_{Cu-O}(^2B_1) < R_{Cu-O}(^2B_2) < R_{Cu-O}(^2A_2)$ (see Table 2).

For all electronic states, except the $^2B_1$ one, the T_1 diagnostic,[58] which is an indication of the quality of the CCSD wave function, is smaller than 0.02. Thus, these states do not show significant multireference character and the CCSD(T) results are expected to be very accurate. For the $^2B_1$ state, the T_1 value is 0.026 and so nondynamic correlation is somewhat more important. Single point energy calculations at the CASPT2/B1 level, based on a $(13,14)$[59] active space and using the CCSD(T)/B1 optimized geometries, provide relative energies of $^2B_1$ and $^2B_2$ with respect to the $^2A_1$ electronic state of 7.5 and

13.6 kcal/mol, respectively.[60] These values are very similar to the CCSD(T) ones (5.6 and 13.7 kcal/mol), which confirm the relative order found at this level of theory.

Results with different density functional methods, however, vary significantly depending on the amount of exact exchange mixed in the functional. First, it should be mentioned that for the $^2B_1$ state and with G96LYP and BLYP the C_{2v} symmetry structure is not found to be a minimum on the potential energy surface but is a first-order saddle point. Symmetry relaxation following the transition vector (b_1) led to a C_s symmetry structure of a $^2A'$ electronic state, with H_2O being somewhat pyramidalized. Moreover, with B3LYP and also with MPW1PW91, in addition to the $C_{2v}(^2A_1)$ and $C_{2v}(^2B_1)$ minima, we have located a $C_s(^2A')$ symmetry structure lower in energy, as found in the previous study of El-Nahas[17] with B3LYP. The stabilization gained upon pyramidalization is, however, small, so we will mainly focus on the relative stabilities of the different electronic states assuming C_{2v} symmetry.

The most striking difference observed between the different functionals is the relative energy of $^2B_1$ with respect to $^2A_1$, which ranges from −9.8 for BLYP to +6.9 for BHLYP with the larger basis set. Thus, for nonhybrid density functional methods, and assuming C_{2v} symmetry, $^2B_1$ is computed to be the lowest electronic state of $Cu^{2+}-H_2O$, whereas with the hybrid BHLYP the ground state is the $^2A_1$ one, as predicted by the CCSD(T) and CASPT2 levels of theory. Note that with the popular B3LYP method the $^2B_1$ state is also wrongly predicted to be lower than the $^2A_1$ one, although with this functional the two states become much closer in energy than with BLYP. Relative energies of the $^2B_2$ and $^2A_2$ states with respect to $^2A_1$ also show significant variations upon increasing the exact HF exchange mixing in the functional. However, changes are not as pronounced as for $^2B_1$, and their relative order is maintained. It can be observed in Table 1 that, among all the functionals considered, the one that provides better results compared to

TABLE 3: Parameter Sets Employed for B3LYP Calculations

parameter set	a_o	a_x	a_c
0[a]	0.000	1.000	1.000
1	0.100	0.900	0.900
2	0.200	0.800	0.800
3	0.300	0.700	0.700
4	0.400	0.600	0.600
5	0.500	0.500	0.500
6	0.600	0.400	0.400
7	0.700	0.300	0.300
8	0.800	0.200	0.200
9	0.900	0.100	0.100

[a] This parameter set corresponds to BLYP functional.

CCSD(T) is the BHLYP one, in which the exact exchange mixing is 50%.

With respect to the geometric parameters, Table 2 shows that the changes of the R_{Cu-O} distance are especially important in the $^2B_1$ electronic state, with the obtained value with the larger basis set ranging from 1.97 Å with BLYP or G96LYP to 1.85 Å with BHLYP. That is, in this electronic state, the metal−ligand distance decreases as much as 0.12 Å upon increasing the percentage of exact exchange in the functional. In the other electronic states, changes are much smaller (<0.03 Å). For the $^2B_1$ state, results with the smaller basis set show that the density functional method that provides geometric parameters in closer agreement with CCSD(T) is the BHLYP one.

To analyze these energetic and structural changes further, we have calculated the different electronic states of Cu^{2+}−H$_2$O by varying monotonically the proportion of exact exchange introduced. We have made use of the Gaussian 98 program feature that allows one to vary the B3LYP standard Becke parameter set (PS) through internal options.[61] In Table 3, we show the different PSs {a_o,a_x,a_c} employed. We have changed the a_o parameter by 0.100 increments in the interval 0.100 ≤ a_o ≤ 0.900, with fixed $a_x = 1 - a_o$ and $a_c = a_x$. The $a_x = 1 - a_o$

relationship has already been used in some hybrid functionals,[62,63] such as the B1 method,[63] which in addition takes $a_c = 1$ and $a_o = 0.16$ or 0.28 depending on the choice of the gradient corrected exchange and correlation functionals in DFT [the so-called generalized gradient approximations (GGA)]. We also found in previous works[27,28] that the $a_x = 1 - a_o$ and $a_c = a_x$ relations between the B3LYP parameters are, on average, the optimal ones to minimize the difference between the actual B3LYP density and the QCISD one in a series of small molecules. For this reason the $a_x = 1 - a_o$ and $a_c = a_x$ relationships will be maintained throughout this work. However, neither the choice that we have employed here nor other possible alternative relations among the three parameters should be considered as universal.[28,62]

The obtained relative energies and optimized geometric parameters as a function of a_o are collected in Tables 4 and 5, respectively. The HF values have been included in these tables for comparison. First, it is worth noting that, for the $^2B_1$ state with $a_o = 0.1$ and the $^2A_1$ state with a_o parameters of 0.3 and 0.4, the C_{2v} structure was found to be a first-order saddle point. This is in agreement with the previous BLYP and G96LYP results for the $^2B_1$ state, which determined the C_{2v} structure to be unstable and evolve to a $^2A'$ state of C_s symmetry.

It can be seen in Table 4 that the ground state of Cu^{2+}−H$_2$O changes from $^2B_1$ to $^2A_1$ between $a_o = 0.2$ and 0.3. The PSs that give the closest results to the CCSD(T) values are those having a_o values of 0.4 and 0.5. Probably an intermediate value of $a_o = 0.45$ will practically reproduce the CCSD(T) relative energies. Increasing the a_o value reduces the stability of $^2B_1$ and increases the stability of the $^2B_2$ and $^2A_2$ electronic states with respect to the $^2A_1$ state. As a consequence, the energy difference between the most and least stable states is reduced from 38.5 to 13.3 kcal/mol when going from $a_o = 0$ (BLYP) to $a_o = 0.9$. Surprisingly, the HF method outperforms most DFT functionals as far as the energy difference between the $^2A_1$ and $^2B_1$ states is concerned.

TABLE 4: Relative Energies (in kcal/mol) of the Ground and Low-Lying Electronic States of C_{2v} Cu^{2+}−H$_2$O Species Computed with the B3LYP Method Using Different Parameter Sets[a] and Basis Set B1[b]

state	parameter set									HF
	1	2	3	4	5	6	7	8	9	
$^2A_1$	0.0	0.0	0.0[c]	0.0[c]	0.0	0.0	0.0	0.0	0.0	0.0
$^2B_1$	−6.6[c]	−2.3	1.9	5.1	6.8	7.4	7.6	7.6	7.5	6.7
$^2B_2$	20.8	18.1	16.0	14.4	13.2	12.2	11.6	11.0	10.6	9.4
$^2A_2$	24.0	20.9	18.7	17.0	15.8	14.9	14.3	13.8	13.3	12.1

[a] See Table 3. [b] HF results have been included for comparison. [c] First-order saddle point. See text.

TABLE 5: Optimized Geometric Parameters of C_{2v} Cu^{2+}−H$_2$O Species in Different Electronic States Computed with the B3LYP Method Using Different Parameter Sets[a] and Basis Set B1[b]

state	geometry	parameter set									HF
		1	2	3	4	5	6	7	8	9	
$^2A_1$	R_{Cu-O}	1.861	1.850	1.845	1.843	1.843	1.844	1.846	1.847	1.848	1.875
	R_{O-H}	0.993	0.987	0.981	0.975	0.970	0.966	0.962	0.958	0.954	0.962
	α_{CuOH}	123.3	124.0	124.6	125.0	125.3	125.5	125.7	125.8	125.9	126.1
$^2B_1$	R_{Cu-O}	1.959	1.925	1.895	1.874	1.870	1.875	1.879	1.883	1.886	1.913
	R_{O-H}	1.003	0.996	0.988	0.980	0.973	0.967	0.962	0.958	0.954	0.962
	α_{CuOH}	126.1	126.2	126.2	126.2	126.2	126.2	126.3	126.3	126.3	126.4
$^2B_2$	R_{Cu-O}	1.913	1.915	1.917	1.917	1.917	1.917	1.917	1.918	1.918	1.942
	R_{O-H}	0.992	0.985	0.979	0.974	0.969	0.965	0.961	0.957	0.953	0.961
	α_{CuOH}	126.2	126.0	126.0	126.0	126.1	126.2	126.3	126.2	126.3	126.4
$^2A_2$	R_{Cu-O}	1.926	1.924	1.922	1.921	1.920	1.920	1.921	1.921	1.921	1.945
	R_{O-H}	0.986	0.982	0.977	0.972	0.968	0.964	0.959	0.955	0.952	0.960
	α_{CuOH}	125.3	125.5	125.7	125.8	126.0	126.1	126.1	126.2	126.3	126.3

[a] See Table 3. [b] Distances are in angstroms and angles are in degrees. HF results have been included for comparison.

6076 *J. Phys. Chem. A, Vol. 108, No. 28, 2004*

Poater et al.

TABLE 6: Delocalization Indices (au) between the Cu and O Atoms, δ(Cu,O), Computed at the B3LYP Level Using Different Parameter Sets[a] and Basis Set B1[b]

| state | parameter set | | | | | | | | | | HF |
	0	1	2	3	4	5	6	7	8	9	
$^2A_1$	0.802	0.767	0.725	0.681	0.640	0.603	0.571	0.543	0.519	0.498	0.475
$^2B_1$	0.904	0.899	0.886	0.846	0.759	0.654	0.579	0.531	0.498	c	0.450
$^2B_2$	0.695	0.630	0.586	0.554	0.528	0.504	0.483	0.464	0.446	0.431	0.418
$^2A_2$	0.657	0.628	0.600	0.574	0.550	0.527	0.506	0.486	0.468	0.451	0.439

[a] See Table 3. [b] HF results have been included for comparison. [c] For this parameter set and electronic state, the AIMPAC numerical integration yields wrong results.

TABLE 7: Interaction Energies for the $^2A_1$ State of $Cu^{2+}-H_2O$ (in kcal/mol) with Basis Sets B1 and B2[a]

	G96LYP	BLYP	B3LYP	MPW1PW91	BHLYP	CCSD(T)[b]
D_e	122.1 (122.0)	124.4 (124.3)	115.8 (115.9)	112.8 (113.1)	107.4 (107.8)	103.8 (104.2)
D_0	120.6 (120.5)	122.9 (122.9)	113.7 (113.7)	109.6 (106.4)	105.7 (106.2)	102.6
$\Delta H_{298}°$	121.8 (121.7)	124.1 (124.0)	114.9 (114.9)	110.9 (107.7)	106.8 (107.3)	103.9

[a] Basis set B2 in parentheses. [b] Value with the B2 basis set is obtained from single point calculations at the optimized CCSD(T)/B1 geometry.
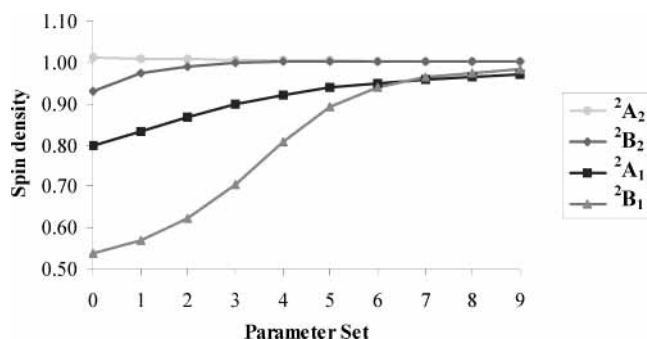

Figure 1. Spin density (au) at the Cu atom for the C_{2v} $Cu^{2+}-H_2O$ species in different electronic states computed with the B3LYP method using different parameter sets (see Table 3) and basis set B1.

With respect to the geometric parameters, for all states, the R_{O-H} bond distance decreases when the fraction of exact HF exchange increases, as expected from the fact that the HF method usually underestimates bond distances. The same effect was found for the H−H bond length in a previous work.[26] The effect on the R_{Cu-O} bond length is more complicated. For the $^2B_1$ and $^2A_1$ electronic states there is a reduction in the Cu−O bond length when increasing the percentage of exact HF exchange until $a_o = 0.5$, and then there is a slight increase. This effect is much more noticeable for the $^2B_1$ than for the $^2A_1$ state. However, the R_{Cu-O} bond length is almost unaffected by the fraction of exact HF exchange included in the modified B3LYP functional for the $^2B_2$ and $^2A_2$ electronic states. These observations appear to be related to the degree of charge and spin delocalization in the different electronic states. This is clearly seen in Figure 1, where the spin density on the Cu atom is depicted as a function of the a_o parameter. For $^2B_1$ the BLYP functional ($a_o = 0$) provides an almost completely delocalized picture, since spin density at the metal atom and water ligand is 0.54 and 0.46, respectively. As the amount of exact HF exchange mixing increases, the spin density becomes more localized at the metal center, with the values ranging from 0.54 for $a_o = 0$ to 0.89 for $a_o = 0.5$. For $a_o > 0.5$ the spin density at Cu slightly increases to 0.98 and for the HF method it is 0.99. In the $^2A_1$ electronic state we observe a similar trend, although the variations are smaller since the spin density ranges from 0.80 to 0.97. However, in the $^2B_2$ and $^2A_2$ electronic states, delocalization is very small, and all PSs provide similar results. The spin density lies almost completely at $Cu^{2+}(d^9)$, and the net atomic charge is very close to 2. Thus, both the $^2B_1$ and $^2A_1$ electronic states are more sensitive to the kind of functional used, especially the $^2B_1$ one for which changes on spin density

are more pronounced. It should be noted that population analysis obtained from UMP4 calculations also provide a localization of the unpaired electron at the metal center, the spin population at Cu^{2+} in the $^2B_1$ and $^2A_1$ states being 0.95 and 0.93, respectively.

The trends in delocalization discussed above from the spin density on Cu can also be analyzed from the delocalization index defined in eq 3. The results obtained for the different states and for all the PSs analyzed are collected in Table 6. HF results are included for comparison. It is seen that (for $a_o < 0.7$) the $^2B_1$ state has the largest degree of delocalization between the Cu and O atoms, followed by the $^2A_1$ state and finally the $^2B_2$ and $^2A_2$ states. It is worth noting that for all states the delocalization decreases when the a_o parameter increases. This is in agreement with previous findings showing that the HF method underestimates the degree of bond delocalization, while pure DFT methods overestimate this delocalization in π conjugated species.[64] The largest δ(Cu,O) delocalization in the $^2B_1$ state compared to $^2A_1$ is due to the fact that there is a small overlap in Cu or O basins between the molecular orbitals corresponding to the bonding and antibonding combination of the metal $(4s-3d_{z^2})(a_1)$ orbital with the $3a_1$ one of H_2O (S_{ij}(A) for these two orbitals in the $^2B_1$ state is ±0.04 at the BLYP level) and a large overlap between the bonding and antibonding combination of the metal $3d_{yz}(b_1)$ with the lone pair $1b_1$ orbital of water H_2O (S_{ij}(A) for these two orbitals in the $^2A_1$ state is ±0.24 at the BLYP level). We have shown in a previous study[56] that the overlap between molecular orbitals has a large influence on the electronic localization and delocalization in open shell systems. For instance, it can be easily shown[56] that adding one electron to the H_2 molecule to form the H_2^- anion increases the global electronic delocalization by $0.5-4$ $S_{\sigma_g\sigma_u*}$(H), where $S_{\sigma_g\sigma_u*}$(H) is the overlap in the basin of a H atom between the σ_g and σ_u* orbitals of H_2. This effect can be generalized, and it is found that when an electron is added to a given species small/large S_{ij}(A) values result in a larger/smaller delocalization.

Now consider the effect on electronic delocalization of adding an electron to the single occupied antibonding a_1* or b_1* orbitals of triplet $Cu^{3+}-H_2O$ to yield the $^2B_1$ or $^2A_1$ electronic states of $Cu^{2+}-H_2O$, respectively. Because of the smaller overlap between the bonding and antibonding orbitals of a_1 symmetry, there is a larger delocalization when adding the electron to the a_1* orbital ($^2B_1$ state) than when adding the same electron to the b_1* orbital ($^2A_1$ state). For this reason, the $^2B_1$ is more delocalized than the $^2A_1$ electronic state. Remarkably, the overlap between the bonding and antibonding combinations of

Ground and Low-Lying States of Cu^{2+}—H$_2$O

J. Phys. Chem. A, Vol. 108, No. 28, 2004 **6077**

a$_1$ symmetry grows when a_o increases up to 0.5 and then remains practically constant,[65] thus explaining the reduction of delocalization in the ^{2}B$_1$ state when a_o increases.

In summary, the results obtained indicate that pure density functionals clearly overestimate the stability of the ^{2}B$_1$ state and provide a delocalized picture of the electron hole. The error is related to the exchange functional, the overstabilization and the degree of delocalization diminishing the more the exchange functional is replaced by exact exchange. On the other hand, the optimized R_{Cu-O} distance in this state appears to be quite sensitive to the functional used; the larger the amount of exact exchange mixing, the smaller the metal—ligand distance (at least until $a_o = 0.5$). This situation is similar to that found in delocalized radical systems (i.e., two center—three electron (3e—2c) bond systems),[21] which present too large interaction energies and too long bond lengths with local density approximation (LDA) or GGA functionals. The overstabilization has been attributed to a bad cancellation of the self-interaction (SI) included in the Coulomb energy by the exchange-correlation functional, due to its delocalized electron hole; the error increases with increasing distance (decreasing overlap between fragment orbitals).[21b]

The overstabilization of the ^{2}A$_1$ ground electronic state is not as important as for ^{2}B$_1$, because the degree of delocalization is smaller. However, it is nonnegligible and it can lead to a too large Cu^{2+}—H$_2$O binding energy. To evaluate how much this important magnitude is affected by the functional used, we have computed the Cu^{2+}—H$_2$O (^{2}A$_1$) interaction energy with the different functionals tested in this work and basis sets B1 and B2. Results are given in Table 7. The values computed with GGA functionals are about 18—20 kcal/mol larger than the CCSD(T) one. Hybrid functionals show smaller deviations (from 12 to 4 kcal/mol), the differences depending on the amount of exact exchange included in the functional; that is, the larger the percentage of HF exchange, the smaller the interaction energy and the better the agreement with CCSD(T). In particular, it is observed that BHLYP provides a Cu^{2+}—H$_2$O interaction energy in good agreement with CCSD(T). Enlarging the basis set from B1 to B2 slightly increases the interaction energy. Since basis set requirements to get a converged value are more important at the CCSD(T) level, we have performed additional calculations by further enlarging the basis set of Cu to [10s7p4d2f1g] and using the aug-cc-VTZ basis[67] set for O and H at this level of theory. The computed CCSD(T) value of D_e with this basis is 107.7 kcal/mol, which is our best estimate for the binding energy of Cu^{2+}—H$_2$O.

IV. Conclusions

The ground and low-lying states of Cu^{2+}—H$_2$O have been studied using different density functional and post-Hartree—Fock methods. At the CCSD(T) level, Cu^{2+}—H$_2$O presents C_{2v} symmetry and the ground electronic state is a ^{2}A$_1$ state. Moreover, at this level of theory the relative order of the electronic states is ^{2}A$_1$ < ^{2}B$_1$ < ^{2}B$_2$ < ^{2}A$_2$. However, density functional results show that the relative stability of these states varies depending on the degree of mixing of exact HF and DFT exchange functionals. For GGA and also for hybrid functionals with low percentages of HF mixing (up to 20—25%), the ^{2}B$_1$ state becomes more stable than the ^{2}A$_1$ one. Moreover, with these functionals a $C_s(^2$A$')$ structure is found to be the ground-state structure of Cu^{2+}—H$_2$O.

These changes are related to the charge and spin delocalization in the different electronic states. For $C_{2v}(^2$B$_1)$ and $C_s(^2$A$')$, GGA functionals provide a delocalized picture of the electron hole, whereas in the $C_{2v}(^2$A$_1)$ state the hole is more localized at the metal atom. Since delocalized situations are overstabilized by LDA and GGA functionals, due to an overestimation of the self-interaction part by the exchange-correlation functional,[21] the $C_{2v}(^2$B$_1)$ or $C_s(^2$A$')$ are wrongly predicted to be lower in energy than the $C_{2v}(^2$A$_1)$ by certain functionals. The admixture of exact exchange reduces the error, the degree of delocalization and overstabilization diminishing the more the exchange functional is replaced by exact exchange. It is found that 40—50% mixing provides results in very good agreement with CCSD(T). Therefore, density functional calculations should be taken with some caution upon comparing situations with different spin distributions.[68]

References and Notes

(1) (a) *The Encyclopedia of Mass Spectrometry. Volume 1: Theory and Ion Chemistry*, Armentrout, P. B., Ed.; Elsevier: Amsterdam, 2003. (b) *Organometallic Ion Chemistry*, Freiser, B. S., Ed.; Kluwer Academic Publishers: Dordrecht, 1996.

(2) (a) Castleman, A. W., Jr.; Bowen, K. H., Jr. *J. Phys. Chem.* **1996**, *100*, 12911. (b) Duncan, M. A. *Annu. Rev. Phys. Chem.* **1997**, *48*, 69. (c) Rodgers, M. T.; Armentrout, P. B. *Mass. Spectrom. Rev.* **2000**, *19*, 215.

(3) Stace A. J. *J. Phys. Chem. A* **2002**, *106*, 7993.

(4) Jayaweera, P.; Blades, A. T.; Ikonomou, M. G.; Kebarle, P. *J. Am. Chem. Soc.* **1990**, *112*, 2452.

(5) Schröder, D.; Schwarz, H. *J. Phys. Chem. A* **1999**, *103*, 7385.

(6) Shvartsburg, A. A.; Michael Siu, K. W. *J. Am. Chem. Soc.* **2001**, *123*, 10071.

(7) See, for example: (a) Bauschlicher, C. W.; Langhoff, S. R.; Partridge, H. *Adv. Ser. Phys. Chem.* **1995**, *2*, 1280. (b) Bauschlicher, C. W. In *Encyclopedia of Computational Chemistry*; Schleyer, P. v. R, Ed.-in-Chief; John Wiley & Sons: Chichester, 1998; Vol. 5, p 3084.

(8) Koch, W.; Holthausen, M. C. *A Chemist's guide to density functional theory*; Wiley-VCH: Weinheim, 2001.

(9) (a) Koch, W.; Hertwig, R. H. *Encyclopedia of Computational Chemistry*; Schleyer, P. v. R, Ed.-in-Chief; John Wiley & Sons: Chichester, 1998; Vol. 1, p 689.

(10) (a) Blomberg, M. R. A.; Siegbahn, P. E.; Svensson, M. *J. Chem. Phys.* **1996**, *104*, 9546. (b) Barone, V.; Adamo, C.; Mele, F. *Chem. Phys. Lett.* **1996**, *249*, 290. (c) Holthausen, M. C.; Mohr, M.; Koch, W. *Chem. Phys. Lett.* **1995**, *240*, 245. (d) Sodupe, M.; Branchadell, V.; Rosi, M.; Bauschlicher, C. W. *J. Phys. Chem. A* **1997**, *101*, 7854. (e) Luna, A.; Alcami, M.; Mo, O.; Yáñez, M. *Chem. Phys. Lett.* **2000**, *320*, 129. (f) Bauschlicher, C. W.; Ricca, A.; Partridge, H.; Langhoff, S. R. In *Recent Advances in Density Functional Theory, Part II*; Chong, D. P., Ed.; World Scientific Publishing Co.: Singapore, 1997.

(11) Trachtman, M.; Markham, G. D.; Glusker, J. P.; George, P.; Bock, C. W. *Inorg. Chem.* **1998**, *37*, 4421.

(12) (a) Ricca, A.; Bauschlicher, C. W. *J. Phys. Chem. A* **2002**, *106*, 3219. (b) Beyer, M.; Williams, E. R.; Bondybey V. E. *J. Am. Chem. Soc.* **1999**, *121*, 1565. (c) Alcami, M.; González, A. I.; Mo, O.; Yáñez, M. *Chem. Phys. Lett.* **1999**, *307*, 244. (d) Marino, T.; Russo, N.; Toscano, M. *J. Mass Spectrom.* **2002**, *37*, 786. (e) Bertran, J.; Rodríguez-Santiago, L.; Sodupe, M. *J. Phys. Chem. B* **1999**, *103*, 2310. (f) Corral, I.; Mo, O.; Yañez, M.; Scott, A. P.; Radom, L. *J. Phys. Chem. A* **2003**, *107*, 10456.

(13) (a) Schröder, D.; Bärsch, S.; Schwarz, H. *J. Phys. Chem. A* **2000**, *104*, 5101. (b) Schröder, D.; Engeser, M.; Schwarz, H.; Harvey, J. N. *Chem. Phys. Chem.* **2002**, *3*, 584.

(14) Stace, A. J.; Walker, N. R.; Wright, R. R.; Firth, S. *Chem. Phys. Lett.* **2000**, *329*, 173.

(15) El-Nahas, A. M. *Chem. Phys. Lett.* **2000**, *329*, 176.

(16) Stace, A. J.; Walker, N. R.; Firth, S. *J. Am. Chem. Soc.* **1997**, *119*, 10239.

(17) (a) El-Nahas, A. M.; Tajima, N.; Hirao, K. *Chem. Phys. Lett.* **2000**, *318*, 333. (b) El-Nahas, A. M. *Chem. Phys. Lett.* **2001**, *345*, 325.

(18) Schröder, D.; Schwarz, H.; Wu, J.; Wesdemiotis, C. *Chem. Phys. Lett.* **2001**, *343*, 258.

(19) Stone, J. A.; Vukomanovic, D. *Chem. Phys. Lett.* **2001**, *346*, 419.

(20) Irigoras, A.; Elizalde, O.; Silanes, I.; Fowler, J. E.; Ugalde, J. M. *J. Am. Chem. Soc.* **2000**, *122*, 114.

(21) (a) Braïda, B.; Hiberty, P. C.; Savin, A. *J. Phys. Chem. A* **1998**, *102*, 7872. (b) Sodupe, M.; Bertran, J.; Rodríguez-Santiago, L.; Baerends, E. J. *J. Phys. Chem. A* **1999**, *103*, 166. (c) Chermette, H.; Ciofini, I.; Mariotti, F.; Daul, C. *J. Chem. Phys.* **2001**, *115*, 11068.

(22) Poater, J.; Solà, M.; Duran, M.; Robles, J. *Phys. Chem. Chem. Phys.* **2002**, *4*, 722.

(23) Latajka, Z.; Bouteiller, Y.; Scheiner, S. *Chem. Phys. Lett.* **1995**, *234*, 159. Lundell, J.; Latajka, Z. *J. Phys. Chem. A* **1997**, *101*, 5004.

(24) Chermette, H.; Razafinjanahary, H.; Carrion, L. *J. Chem. Phys.* **1997**, *107*, 10643.

(25) Hoe, W.-M.; Cohen, A. J.; Handy, N. C. *Chem. Phys. Lett.* **2001**, *341*, 319.

(26) Csonka, G. I.; Nguyen, N. A.; Kolossváry, I. *J. Comput. Chem.* **1997**, *18*, 1534.

(27) Solà, M.; Forés, M.; Duran, M. In *Advances in Molecular Similarity*; Carbó, R., Mezey, P., Eds.; JAI Press: New York, 1998; Vol. 2, p 187.

(28) Poater, J.; Duran, M.; Solà, M. *J. Comput. Chem.* **2001**, *22*, 1666.

(29) Durant, J. L. *Chem. Phys. Lett.* **1996**, *256*, 595.

(30) Jursic, B. S. In *Recent Developments and Applications of Modern Density Functional Theory*; Seminario, J. M., Ed.; Elsevier Science: Amsterdam, 1996; p 709.

(31) Lynch, B. J.; Fast, P. L.; Harris, M.; Truhlar, D. G. *J. Phys. Chem. A* **2000**, *104*, 4811. Lynch, B. J.; Truhlar, D. J. *J. Phys. Chem. A* **2001**, *105*, 2936.

(32) Kormos, B. L.; Cramer, C. J. *J. Phys. Org. Chem.* **2002**, *15*, 712.

(33) Abu-Awwad, F.; Politzer, P. *J. Comput. Chem.* **2000**, *21*, 227.

(34) Dkhissi, A.; Alikhani, M. E.; Boutellier, Y. *J. Mol. Struct. (THEOCHEM)* **1997**, *416*, 1.

(35) Wilson, P. J.; Tozer, D. J. *J. Chem. Phys.* **2002**, *116*, 10139.

(36) Reiher, M.; Salomon, O.; Hess, B. A. *Theor. Chem. Acc.* **2001**, *107*, 48.

(37) Bartlett, R. J. *Annu. Rev. Phys. Chem.* **1981**, *32*, 359.

(38) Raghavachari, K.; Trucks, G. W.; Pople, J. A.; Head-Gordon, M. *Chem. Phys. Lett.* **1989**, *157*, 479.

(39) Wachters, A. J. H. *J. Chem. Phys.* **1970**, *52*, 1033.

(40) Hay, P. J. *J. Chem. Phys.* **1977**, *66*, 4377.

(41) Raghavachari, K.; Trucks, G. W. *J. Chem. Phys.* **1989**, *91*, 1062.

(42) Lee, C.; Yang, W.; Parr, R. G. *Phys. Rev. B* **1988**, *37*, 785.

(43) Becke, A. D. *Phys. Rev. A* **1988**, *38*, 3098.

(44) Gill, P. M. W. *Mol. Phys.* **1996**, *89*, 433.

(45) Becke, A. D. *J. Chem. Phys.* **1993**, *98*, 5648.

(46) Becke, A. D. *J. Chem. Phys.* **1993**, *98*, 1372.

(47) (a) Perdew, J. P. In *Electronic Structure of Solids '91*; Ziesche, P., Eschrig, H., Eds.; Akademie Verlag: Berlin, 1991; p 11. (b) Perdew, J. P.; Chevary, J. A.; Vosko, S. H.; Jackson, K. A.; Pederson, M. R.; Singh, D. J.; Fiolhais, C. *Phys. Rev. B* **1992**, *46*, 6671; *Phys. Rev. B* **1993**, *48*, 4978-(E). (c) Perdew, J. P.; Burke, K.; Wang, Y. *Phys. Rev. B* **1996**, *54*, 16533; *Phys. Rev. B* **1998**, *57*, 14999(E).

(48) Frisch, M. J.; Trucks, G. W.; Schlegel, H. B.; Scuseria, G. E.; Robb, M. A.; Cheeseman, J. R.; Zakrzewski, V. G.; Montgomery, J. A., Jr.; Stratmann, R. E.; Burant, J. C.; Dapprich, S.; Millam, J. M.; Daniels, A. D.; Kudin, K. N.; Strain, M. C.; Farkas, O.; Tomasi, J.; Barone, V.; Cossi, M.; Cammi, R.; Mennucci, B.; Pomelli, C.; Adamo, C.; Clifford, S.; Ochterski, J.; Petersson, G. A.; Ayala, P. Y.; Cui, Q.; Morokuma, K.; Malick, D. K.; Rabuck, A. D.; Raghavachari, K.; Foresman, J. B.; Cioslowski, J.; Ortiz, J. V.; Baboul, A. G.; Stefanov, B. B.; Liu, G.; Liashenko, A.; Piskorz, P.; Komaromi, I.; Gomperts, R.; Martin, R. L.; Fox, D. J.; Keith, T.; Al-Laham, M. A.; Peng, C. Y.; Nanayakkara, A.; Gonzalez, C.; Challacombe, M.; Gill, P. M. W.; Johnson, B.; Chen, W.; Wong, M. W.; Andres, J. L.; Gonzalez, C.; Head-Gordon, M.; Replogle, E. S.; Pople, J. A. *Gaussian 98*; Gaussian, Inc.: Pittsburgh, PA, 1998.

(49) Stephens, P. J.; Devlin, F. J.; Chabalowski, C. F.; Frisch, M. J. *J. Phys. Chem.* **1994**, *98*, 11623.

(50) Vosko, S. J.; Wilk, L.; Nusair, M. *Can. J. Phys.* **1980**, *58*, 1200. Hertwig, R. H.; Koch, W. *Chem. Phys. Lett.* **1997**, *268*, 345.

(51) Adamo, C.; Barone, V. *J. Chem. Phys.* **1998**, *108*, 664.

(52) Baerends, E. J.; Branchadell, V.; Sodupe, M. *Chem. Phys. Lett.* **1997**, *265*, 481.

(53) Biegler-König, F. W.; Bader, R. F. W.; Tang, T.-H. *J. Comput. Chem.* **1982**, *3*, 317.

(54) Bader, R. F. W.; Stephens, M. E. *J. Am. Chem. Soc.* **1975**, *97*, 7391.

(55) Fradera, X.; Austen, M. A.; Bader, R. F. W. *J. Phys. Chem. A* **1999**, *103*, 304. Fradera, X.; Poater, J.; Simon, S.; Duran, M.; Solà, M. *Theor. Chem. Acc.* **2002**, *108*, 214.

(56) Fradera, X.; Solà, M. *J. Comput. Chem.* **2002**, *23*, 1347.

(57) Rosi, M.; Bauschlicher, C. W., Jr. *J. Chem. Phys.* **1989**, *90*, 7264.

(58) Lee, T. J.; Taylor, P. R. *Int. J. Quantum Chem.* **1989**, *S23*, 199.

(59) CASSCF active space includes 14 orbitals ($6a_1$, $4b_1$, and $4b_2$), which correspond to combinations of the oxygen 2s and 2p, the hydrogen 1s and the metal 4s and 3d orbitals, except the $3d_{x^2-y^2}$ and $3d_{xy}$ which were moved to the inactive space.

(60) The weight of the main configuration in the CASPT2 calculations for the $^2A_1$, $^2B_1$, and $^2B_2$ states is 0.93, 0.90, and 0.94, respectively.

(61) To do this, one must define the Gaussian route as #B3LYP IOP-($5/45 = P_1P_2$) IOP($5/46 = P_3P_4$) IOP($5/47 = P_5P_6$). The E_{B3LYP} energy is therefore given by $E_{B3LYP} = p_2E_X^{HF} + p_1(p_4E_X^{LDA} + p_3E_X^{B88}) + p_6E_C^{VWN} + p_5(E_C^{LYP} - E_C^{VWN})$, where $p_i = P_i/1000$, for $i = 1-6$. Then relations to Becke's parameters are given by $a_o = p_2$ or $1 - p_1p_4$, $a_x = p_1p_3$, and $a_c = p_5$. p_1 and p_6 have been set equal to 1 in this work. The values $P_1 = 1000$, $P_2 = 200$, $P_3 = 720$, $P_4 = 800$, $P_5 = 810$, and $P_6 = 1000$ reproduce the original B3LYP results.

(62) Burke, K.; Ernzerhof, M.; Perdew, J. P. *Chem. Phys. Lett.* **1997**, *265*, 109.

(63) Becke, A. D. *J. Chem. Phys.* **1996**, *104*, 1040.

(64) King, R. A.; Crawford, T. D.; Stanton, J. F.; Schaefer, H. F., III. *J. Am. Chem. Soc.* **1999**, *121*, 10788. Choi, C. H.; Kertesz, M. *J. Phys. Chem. A* **1998**, *102*, 3429.

(65) The increase of the overlap between bonding and antibonding combinations of a_1 molecular orbitals in the atomic basin of Cu or O when a_o increases is attributed to the reduction of the Cu−O bond. Because of this reduction there is an increase in the overlap (S) between the metal ($4s-3d_{z^2}$) (a_1) orbital and the $3a_1$ one of H_2O. Due to this increase, the coefficients of the ($4s-3d_{z^2}$) (a_1) orbital of the metal and the $3a_1$ orbital of H_2O in the bonding and antibonding molecular orbitals become more similar (the coefficients in these molecular orbitals are related by the approximate expression[66] $c(3a_1) = \pm\{(S/[\epsilon(3a_1) - \epsilon(4s-3d_{z^2})])(c(4s-3d_{z^2}))\}$) and the overlap between bonding and antibonding combinations of a_1 molecular orbitals in the atomic basin of Cu or O becomes larger.

(66) Rauk, A. In *Orbital Interaction Theory of Organic Chemistry*; John Wiley & Sons: New York, 1994; p 72.

(67) Kendall, R. A.; Dunning, T. H.; Harrison, R. J. *J. Chem. Phys.* **1992**, *96*, 6796.

(68) Noguera, M.; Bertran, J.; Sodupe, M. *J. Phys. Chem. A* **2004**, *108*, 333.